Hydrology and Earth System Sciences, 3(1), *109–124* (1999) © EGS

Hydrology & Earth System Sciences

River routing at the continental scale: use of globally-available data and an *a priori* method of parameter estimation

Pam Naden,[1] Peter Broadhurst,[1] Nicholas Tauveron[2] and Alec Walker[3]

[1] Institute of Hydrology, Wallingford, UK
[2] École Polytechnique, Paris, France
[3] University College London, UK

Abstract

Two applications of a river routing model based on the observed river network and a linearised solution to the convective-diffusion equation are presented. One is an off-line application to part of the Amazon basin (catchment area 2.15 M km^2) using river network data from the Digital Chart of the World and GCM-generated runoff at a grid resolution of 2.5 degrees latitude and 3.75 degrees longitude. The other application is to the Arkansas (409,000 km^2) and Red River (124,400 km^2) basins as an integrated component of a macro-scale hydrological model, driven by observed meteorology and operating on a 17 km grid. This second application makes use of the US EPA reach data to construct the river network. In both cases, a method of computing parameter values *a priori* has been applied and shows some success, although some interpretation is required to derive 'correct' parameter values and further work is needed to develop guidelines for use of the method. The applications, however, do demonstrate the possibilities for applying the routing model at the continental scale, with globally-available data and *a priori* parameter estimation, and its value for validating GCM output against observed flows.

Introduction

One of the key datasets for validating global climate models (GCMs) is river flow data from the world's major rivers —catchments of the order of 10,000–100,000 km^2 and above. This is an important source for validation as river flow is an output which represents the integration of all the atmospheric and hydrological processes, including human intervention, operating within a catchment. It also provides an opportunity to assess the terrestrial water balance at a spatial scale similar to that on which GCMs operate (200-300 km grids). While river flow data are not without errors, flow is considerably easier to measure than either evaporation or soil moisture. River flow data are also widely collected as part of national water resources programmes and have been collated through a number of international initiatives, e.g. through the World Climate Programme at the Global Runoff Data Centre (e.g. Dümenil *et al.*, 1993) and through UNESCO under the FRIEND (Flow Regimes for International Experimental and Network Data) programme (Gustard, 1994).

In general, runoff in GCMs, even on an annual basis, is predicted relatively poorly for the world's major drainage basins (e.g. Russell and Miller, 1990, Sausen *et al.*, 1994). In some cases, this is partly due to problems in predicting rainfall but, in many other cases, it is the land-surface scheme which may be at fault. Consequently, to identify where the major problems are and how predictions might subsequently be improved, validation against both precipitation fields and river flow is urgently required. With regard to precipitation, satellite information, such as that produced by the Tropical Rainfall Measuring Mission, is beginning to make this possible on the global scale. In terms of flow, important diagnostics are the seasonality of the estimated runoff, compared to observed flows, and the location within the basin where modelled and estimated runoff diverge. This latter diagnostic can be examined by considering flows at successive downstream gauging points within each major basin. However, to compare anything other than annual volumes, the correct timing and attenuation of runoff is fundamental and so a suitable river routing procedure is required. This should include both within and between grid-box routing, dependent on the time and space scales represented, and, if there is no significant feedback between the routed water and the atmosphere, it may be carried out off-line.

In addition to the important point of validation, river

routing is required to provide the correct timing of freshwater flows into the major oceans for the case of coupled land-atmosphere-ocean models. Given the area drained by some of the world's largest rivers, this can mean a time lag since the generation of runoff of the order of several months, compared to most current practice in which runoff from atmospheric models is input directly and immediately into the oceans. The large wetlands of continental interiors (e.g. the Niger, Senegal, Okavango and Sudd in Africa) also comprise special cases which may be significant for atmospheric fluxes. In general, these are fed by rainfall from outside the immediate area and, therefore, the local evapotranspiration may be increased by the presence of the wetland in an otherwise dry area. An example of the order of magnitude of this effect is the Niger wetlands (Sutcliffe and Parks, 1989) which have a flooded area which varies seasonally between about 2000 and 40,000 km^2 and annual water losses which range from 20×10^9 to 50×10^9 m^3, i.e. from 500 mm up to 1250 mm. This far exceeds the maximum annual regional evapo-transpiration loss during a wet year of only 480 mm, thus illustrating the potential impact of lateral water transfers on the water flux back into the atmosphere. The seasonal pattern of river flows downstream is also dominated by the wetland. In cases such as this, routing of runoff to the wetland, its storage, subsequent losses, and the onward passage of water downstream all have to be modelled, and, because of the feedback with the atmosphere, the routing must be coupled fully into the atmospheric model.

Several routing schemes have been put forward for use with GCMs; these range from simple grid-to-grid advection schemes or series of linear reservoirs (Miller *et al.*, 1994; Sausen *et al.*, 1994; Oki *et al.*, 1996), through those which include simple representations of within-grid routing components (Lohmann *et al.*, 1996; Liston *et al.*, 1994; Nijssen *et al.*, 1997) or floodplain inundation (Vörösmarty, *et al.*, 1989), to those which are more closely linked to the observed river channel network (Naden, 1993). In all cases, estimation of the parameters for global application is an important consideration. This paper develops the network width function approach to river routing (Kirkby, 1976; Mesa and Mifflin, 1986; Naden, 1992) and its application to the continental scale, including the use of globally-available data and methods for parameter estimation. The examples given are an offline GCM validation in the Amazon basin and an application, as part of a macro-scale hydrological model, to the Arkansas and Red River basins in the Mississippi (Kilsby *et al.*, 1999).

The model

Given the requirement for a river-routing component linked to global climate models, key factors are that the model should be capable of using globally-available data; should be computationally efficient (especially if it is to be used in fully-coupled mode); should be physically-based and, therefore, require little calibration. At the continental scale, it is also important that the model should be able to route generated runoff from within each GCM grid box. There are two ways in which this problem can be approached. Either water can be routed from grid box to grid box (e.g. Sausen *et al.*, 1994; Oki *et al.*, 1996), or it can be routed directly from each grid box to the point of interest, whether this is a flow gauging station for validation, an ocean input, or an internal wetland site. The first of these approaches more easily allows for feedback between the routed flow and the water content of each grid box, thus enabling non-linear losses from the channel to the floodplain or aquifer to be included, if appropriate. The second enables more efficient computation and, in the form described here, incorporates within-grid as well as grid-to-point and point-to-point routing elements.

The formulation used may be described as a lumped routing model with distributed inputs. Its physical basis is provided by the observed river network and by the Saint Venant equations for open channel flow which describe the conservation of both mass and momentum at any cross-section within the flow. It is assumed that the movement of water is dominated by the friction, bed slope and pressure slope terms, thus allowing the use of a convective-diffusion approximation (Beven and Wood, 1993). The movement over time of a unit volume of water per unit width of channel added instantaneously to the system at its upstream end ($s = 0$) is described by

$$\frac{\partial q_p}{\partial t} = D\frac{\partial^2 q_p}{\partial s^2} - c\frac{\partial q_p}{\partial s} \qquad (1)$$

with boundary conditions

$$q_p(0,t) = \delta(t)$$
$$q_p(s,0) = 0 \quad \text{for } s > 0$$

where q_p is the perturbation discharge per unit width of channel (m^2s^{-1})
D is a diffusion or attenuation coefficient (m^2s^{-1})
c is a wave velocity (ms^{-1})
s is distance (m)
t is time (s)
δ is the Dirac delta function.

It is also assumed that, for large basins in which the response is slow (days to months), a linearised solution to this equation will be adequate. Assuming c and D to be constant in both space and time, this is given (Eagleson, 1970; van de Nes, 1973) by

$$q_p(s,t) = \frac{s}{2\sqrt{\pi D t^3}} \exp\left[-\frac{(s-ct)^2}{4Dt}\right] \qquad (2)$$

and represents the instantaneous response at distance s and time t to an instantaneous input at time $t = 0$ and distance $s = 0$.

GRID-TO-POINT ROUTING ELEMENT

For the case where the flow derives from a lateral input added over a distance s and time t, the step response function which represents the space-time response of the network to an unending uniform input is derived by integrating Eqn. (2) with respect to both space and time, such that

$$C_{s,t}(s,t) = \int_0^s \int_0^t q(s,t)\, dt\, ds \tag{3}$$

The solution to Eqn. (3) is given by Naden (1992) as

$$C_{s,t}(s,t) = \frac{1}{2}\left[\frac{D}{c}\exp\left(\frac{cs}{D}\right)\operatorname{erfc}\left(\frac{s+ct}{\sqrt{4Dt}}\right) - \frac{D}{c} + s + \left(\frac{2D}{c} + ct\right)\operatorname{erf}\left(\frac{ct}{\sqrt{4Dt}}\right) + \left(\frac{D}{c} - s + ct\right)\operatorname{erf}\left(\frac{s-ct}{\sqrt{4Dt}}\right) - \sqrt{\frac{4Dt}{\pi}}\left(\exp\left(-\frac{s-ct}{\sqrt{4Dt}}\right)^2 - \exp\left(-\frac{c^2t}{4D}\right)\right)\right] \tag{4}$$

where erf$z$ is the error function
erfc z is the complementary error function (Abramowitz & Stegun, 1965).

For input over discrete space and time steps, Δs and Δt, the instantaneous response at point (s,t) is then given by subtracting replicas of the step response function, given by Eqn. (3), offset by time Δt and space Δs, and scaling to unit volume. To deal with a network of channels, this response also needs to be weighted by the number of channels contributing at successive distances away from the point of interest. These weights are derived from mapped blue line data in the form of a network width function (Kirkby, 1976). The normalised network width function (NNWF) is simply the number of channel crossings at successive distances along the network upstream from the point of interest, expressed as a proportion of the total number of channel crossings over the whole network. It represents the spatial layout of the channels and provides a measure of the geomorphological dispersion (Rinaldo *et al.*, 1991; Snell and Sivapalan, 1994) of the channel flow. The instantaneous response function for the network as a whole at the downstream outlet is then given by

$$NRF(t) = \frac{1}{\Delta s\, \Delta t}\sum_{n=1}^{m} NNWF_n[C(n\Delta s, t) - C((n-1)\Delta s, t) - C(n\Delta s, (t-\Delta t)) + C((n-1)\Delta s, (t-\Delta t))] \tag{5}$$

where $NRF(t)$ is the network response function
$NNWF_n$ is the normalised network width function at n space increments from the outlet
m is the maximum number of space increments in the network width function.

This response function is convolved with the generated runoff to provide the outflow at the point of interest. This gives continuous output at the outflow point for a stepped lateral input. For flow calculated over discrete time intervals, the function should be integrated over time to provide volumes of flow during those time intervals (Todini, 1996).

POINT-TO-POINT ROUTING ELEMENT

In the case of outflow from interior wetlands or for the case of validation against nested catchments, it is also necessary or expedient to route water from a single inflow point down the main channel as well as dealing with the lateral input to the channels within the area. In this case, the convective-diffusion Eqn. (2) needs only to be integrated over time to give the instantaneous response function for a step input at the upstream end of the main stem. The step response function is, therefore, given by

$$C_t(s,t) = \int_0^t q(s,t)dt = 0.5\left[\exp\left(\frac{cs}{D}\right)\operatorname{erfc}\left(\frac{s+ct}{\sqrt{4Dt}}\right) + \operatorname{erfc}\left(\frac{s-ct}{\sqrt{4Dt}}\right)\right] \tag{6}$$

and the channel response function for a main stem of length s and a step input over period Δt is given by

$$CRF(t) = \frac{1}{\Delta t}\left[C_t(s,t) - C_t(s,t+\Delta t)\right] \tag{7}$$

COMMENT

It is important to realise that this method of river routing is designed fundamentally to route water from an area directly to a point. As seen above, the chain can be broken to incorporate specific features where water can accumulate and interact with the surrounding land/atmosphere. However, for the simple case where there is no feedback, the method is volume conserving and routing is not sequential. Methods for accommodating water losses in this type of approach have been developed by Franchini and Todini (1989); these can be applied in cases where the loss is constant or a function of the surrounding land surface but is independent of the flow. In cases where losses are a function of the flow, the linearity assumption of the method no longer holds and alternative formulations should be used.

In addition to the simplicity and computational efficiency of the method, it has the advantage of being physically based (Franchini and O'Connell, 1996) and, under certain assumptions, the two parameters c and D can be related to channel geometry (see below). Unlike simple

grid-to-grid advective schemes, it also includes, explicitly, the dispersion of the flood wave and the use of the observed river network constrains the model parameters to physically-realistic values. For example, the parameter D properly describes the hydraulic diffusion and does not also have to subsume the geomorphological dispersion as this is included through the network width function. Similarly, the velocity, expressed in parameter c, relates to the mapped distance along the river network and not to an *ad hoc* straight line distance between grid cells. While it is appreciated that both the mapped distance and the *precise* detail of the network width function are related to the map scale used (Naden, 1993), it is anticipated that simple adjustment factors might be developed to accommodate this, if necessary.

Derivation of parameters *a priori*

As the method described above is physically-based, then there is an inbuilt relationship between the parameters c and D, and the geometry of the flow (Dooge, 1973). This is described by the relations:

$$c = \frac{3}{2}v_0; \quad D = \frac{q_0}{2S_0}\left(1 - \frac{F_0^2}{4}\right) \tag{8}$$

where v_0 is the steady state reference velocity (ms^{-1})
S_0 is the energy slope (approximated by the channel bed slope)
q_0 is the steady state reference discharge per unit width (m^2s^{-1})
F_0 is the Froude number.

However, these relations only hold under the assumption of a uniform channel. In the case of large river basins, the channel geometry changes downstream and so, under the lumped formulation developed above, c and D must be considered to be *effective* parameters. It is also known that channel geometry changes in a consistent fashion downstream and, therefore, hydraulic geometry relations (Leopold and Maddock, 1953) may be used to estimate these effective parameters. A method for doing this has been formulated by Snell and Sivapalan (1995) and followed up by Robinson *et al.* (1995). This makes the assumptions of steady state, gradually-varied flow, negligible variation in velocity over the cross-section and uniform roughness height. Use is then made of both downstream and at-a-station hydraulic geometry relationships, and a regional flood relationship, which describes the variation of flood discharge with catchment area for a constant return period. The effective wave velocity is calculated using a weighted harmonic mean of the wave velocities in all reaches – essentially a mean travel time. The effective diffusion coefficient is calculated using a simple weighted arithmetic mean. Assuming a homogeneous rainfall distribution and a rectangular network width function, the resulting equations for the effective values of c and D are

$$c = \frac{\left\{1 - [1 - (b_1 + f_1) - \theta((b_2 - b_1) + (f_2 - f_2))] / \phi_3\right\}^2}{\left[(b_1 + f_1)a_2c_2\psi^{[(b_2-b_1)+(f_2-f_1)]}\right]} \cdot A^{[1-(b_1+f_1)-\theta(b_2-b_1)+(f_2-f_1)]} \cdot p_0^{[1-(b_1+f_1)]} \tag{9}$$

$$D = \frac{\left(2\alpha a_2\psi^{(b_2-b_1)}\right)^{-1}}{\left[(1 - b_1 - \theta(b_2 - b_1) - \beta) / \phi_3 + 1\right]^2} \cdot A^{[1-b_1-\theta(b_2-b_1)-\beta]} \cdot p_0^{(1-b_1)} \tag{10}$$

where b_1 is at-a-site width exponent
b_2 is downstream width exponent
a_2 is downstream width scaling coefficient
f_1 is at-a-site depth exponent
f_2 is downstream depth exponent
c_2 is downstream depth scaling coefficient
θ is regional discharge area exponent
ψ is regional discharge area coefficient
ϕ_3 is maximum network path length exponent
β is link slope exponent
α is link slope coefficient
A is catchment area (m^2)
p_0 is effective rainfall rate (ms^{-1}).

These equations are applied below, with limited published data, to both the Amazon, and the Arkansas and Red River basins.

Application of the method to continental-scale basins

The routing method described above has been applied previously, with some success, to the case of catchments of the order of 10,000 km^2 in the UK using digitised river network data from both 1:50k and 1:250k Ordnance Survey maps (Naden, 1993). This paper focuses on applications at the continental scale.

AMAZON BASIN

In the case of the Amazon basin, the use of globally-available data with GCM output was tackled and so this provides an example of an off-line application for the purpose of validating GCM output against river flow data. The Amazon is the largest river basin in the world with an area of around 7,050,000 km^2 and a mainstream channel length of some 6,516 km (van der Leeden *et al.*, 1990). The example given here is for the lowest site with flow data at Manacapurú, which drains an area of 2.15 M km^2 and has a mainstream length of 4,617 km. Manacapurú is on the Rio Solimões, upstream of the confluence where the Rio Solimões and the Rio Negro combine to form the River Amazon.

Available data

The river network data used were provided on CD ROM from the Digital Chart of the World at a scale of 1:1M (DCW; Denko, 1992). Morley and Walker (pers.comm.) have assessed the accuracy of these data for the derivation of catchment boundaries and river networks at a catchment scale of 10,000 km^2 in the UK. They concluded that using the blue lines depicting watercourses is adequate, even at this relatively small scale, for representing the main river network structure, and hence the definition of the network width function. However, the digital elevation data on the DCW are digitised contour lines at 1000 foot contour intervals supplemented by triangulated spot heights and contours at 250 foot intervals below 1000 feet. Gridded elevations at a scale of 1 km derived from these data were not detailed enough for the definition of catchment boundaries except when used in association with the blue line data. Other inaccuracies in the DCW data themselves have also been noted—in particular, the difference in drainage density between adjacent map sheets. However, at the scale of the Amazon, this sort of inaccuracy is relatively unimportant.

The DCW river network data consist of unstructured river segments, i.e. they have no downstream connectivity. Many groups are currently involved in improving the DCW dataset and a partly cleaned-up version was made available in Arc/Info format through the USGS EROS Data Centre and University College London. The dataset for the Amazon comprises over 60,000 arcs and is held in 33 half degree blocks. However, these data had to be substantially edited to produce a dataset which could be used to generate a network width function. The requirement for this is a topologically-structured set of *single* channels. To provide continuity across the boundaries required the snapping of blue lines in adjacent blocks and either adding links or moving links as appropriate. In addition, methods had to be devised for treating mid-channel islands, braids, swamps, wide channels which are represented in the DCW by both banks of the river, and the delta at the mouth of the Amazon.

The methods used were a mixture of manual and automated techniques (Tauveron, 1996), checked against the charts of the US Defence Mapping Agency. It was, for example, necessary to delete specific arcs where basins outside the Amazon were mistakenly connected (e.g. the Rio Chiquicara flows into the Pacific Ocean but, because of the inclusion of the Huarez aquaduct, this also appeared to be a tributary of the Amazon). The smallest mid-channel islands were removed automatically and braided channels were disconnected at their upstream ends. In the case of the large rivers represented by both banks, one of the lines was deleted and the tributaries reconnected to the new single channel. For the delta area, about 300 km in length with numerous large islands, e.g. the Ilha de Marajo is itself about 50,000 km^2, three outlets to the ocean were recognised and connected arcs were edited accordingly. Each of these solutions introduces a slight error in the precise location of the rivers but it is not thought that the changes will significantly affect the overall network width function. Given the problem of defining catchment boundaries from the DCW elevation data, an approximate boundary was added using the buffer command in Arc/Info, with a buffer width of 20 km to avoid a non-convex polygon; a 5% overestimate of the basin area resulted.

For validating GCM output, good river flow data are required. This is a problem for large rivers where slopes are very shallow, control points are limited and backwater effects may extend over considerable distances, leading to significant hysteresis in stage-discharge rating curves. Thus, while water level data exist for a large number of sites in the Amazon basin, reliable flow data are rather limited. Daily flow data for 1 January 1979 to 31 December 1989 for the Rio Solimões at Manacapurú were made available by the Brazilian Departmento Nacional de Águas e Energia Eléctrica (DNAEE) and ORSTOM (Guyot, pers.comm.).

Generated runoff was available on a daily basis from the Hadley Centre control run CBYUNA of the third climate version of the Meteorological Office Forecast/Climate GCM (Hall *et al.*, 1995) for a 10 year period from March 1979 to February 1989. The generated runoff includes both surface runoff and subsurface drainage from the soil and represents the total water lost from the land-atmosphere system. The model uses a 360-day year with appropriate adjustments for the incident radiation. To make comparisons between the GCM output and observed flow data, the last five or six days of observed flow in each year were omitted. Strictly speaking, the observed flow data should have been resampled on a 360/365 or 360/366 interval. However, given the smooth nature of the observed flow hydrograph, the method adopted is not thought to have introduced a significant error. The resolution of the GCM is 2.5 degrees latitude and 3.75 degrees longitude, equivalent to a grid of approximately 280 by 420 km. This provides 63 grid boxes over the entire Amazon basin and 31 grid boxes for the basin to Manacapurú. Figure 1 shows the final network description with the catchment boundary and overlaid grid boxes.

Network width functions were derived for the Amazon to Manacapurú and subdivided according to the GCM grid using a Lambert azimuthal equal area projection. They are shown in Fig. 2a in terms of the number of individual channels against distance from the basin outlet in each of the grid boxes.

Model results

To derive the network response functions, the routing model was calibrated using the first four years of the observed flow data. This provided values of 0.32 ms^{-1} for the wave velocity and 99,500 m^{2}s^{-1} for the diffusion coefficient and a Nash-Sutcliffe efficiency of 53% over

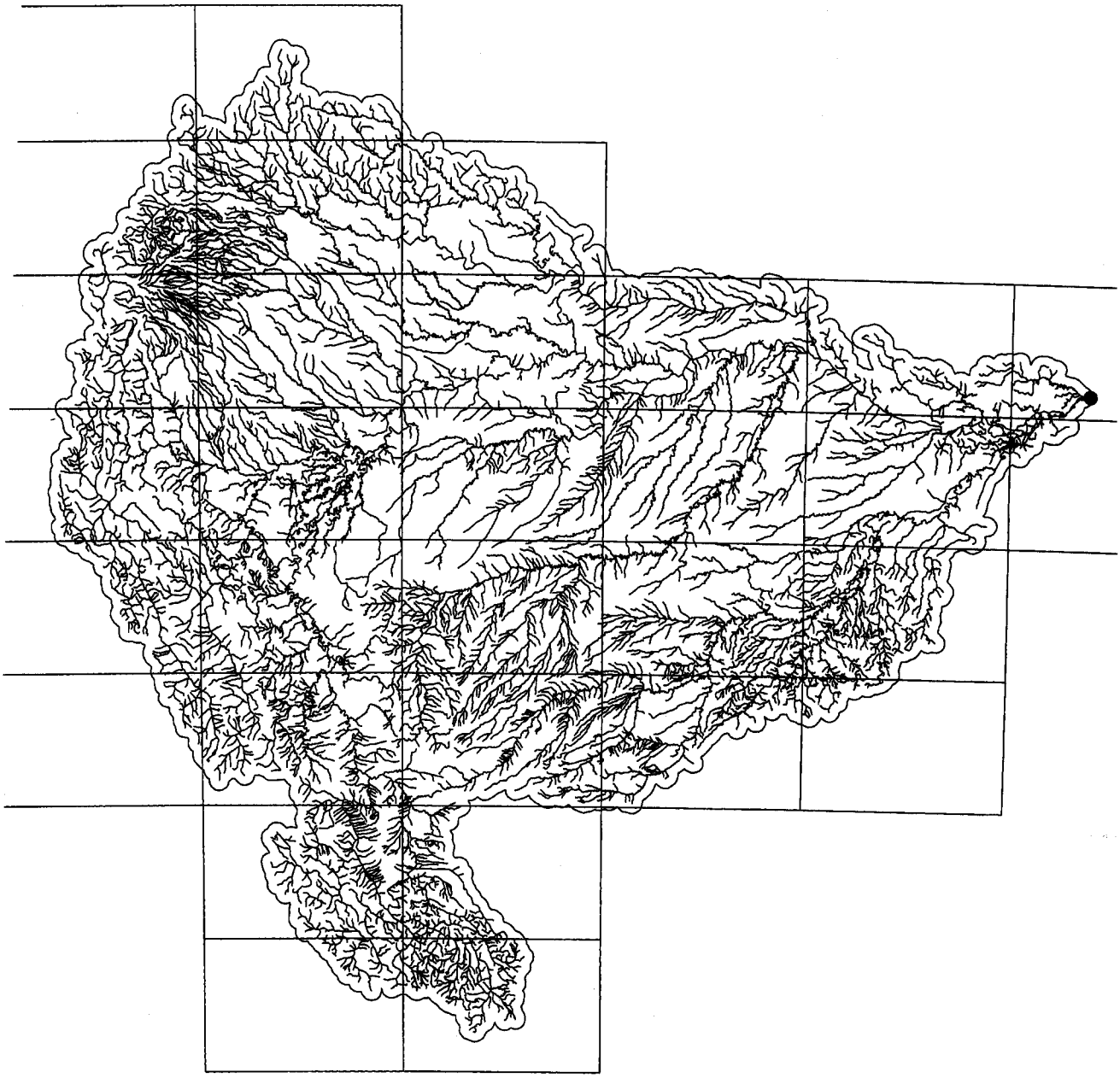

Fig. 1. *River network of the Amazon to Manacapurú (•) showing catchment area defined by Arc/Info 20 km buffer zone and GCM grid squares (2.5 degrees latitude; 3.75 degrees longitude).*

those four years. Much of the cause of the relatively low efficiency is the difference in water volumes between the generated runoff and observed flow rather than the performance of the routing model. As shown in Table 1, the generated runoff underestimates the observed flow by an average of 21%. This is despite overestimating the basin area, which would tend to counteract this bias. The discrepancy is largely due to an underestimation of the amount of rainfall (Cox, pers.comm.). This is similar to findings from other GCM runs such as those shown in Kuhl and Miller (1992), Russel and Miller (1990) and Sausen *et al.* (1994). There is also a tendency for the discrepancy in volumes to increase over the nine-year period.

The calibrated network response functions against time are shown in Fig. 2b. The calibrated value of the kinematic wave velocity (0.32 ms^{-1}) agrees well with figures derived by Richey *et al.* (1989) and Miller *et al.* (1994) and is consistent with the passage of flood peaks down the Amazon as derived from ERS-1 and TOPEX/Poseidon radar altimetry (Birkett, 1998). This value is, however, somewhat less than the 0.42 ms^{-1} calculated from the residence time and grid dimensions used by Vörösmarty *et al.* (1989)

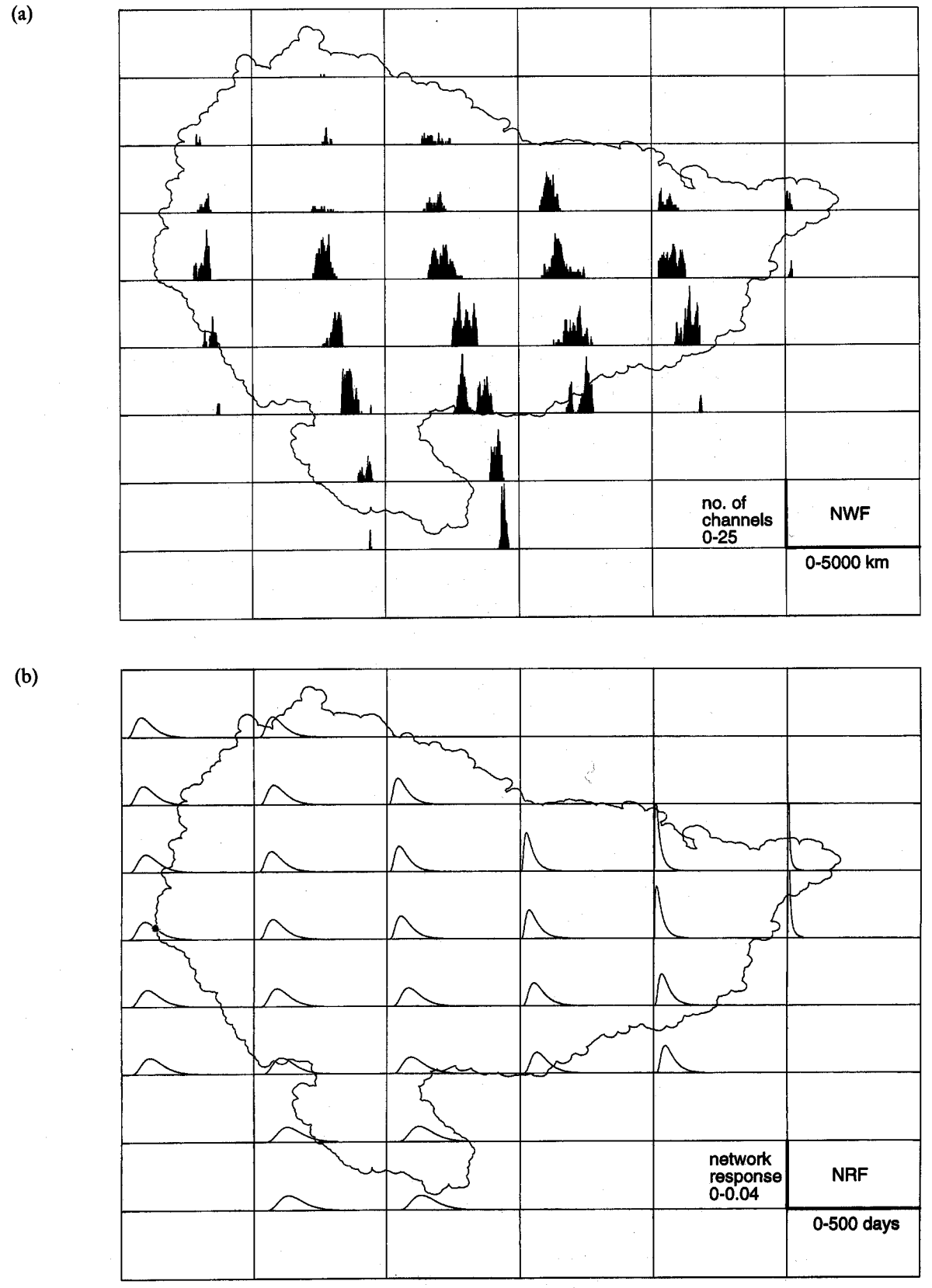

Fig. 2. *Manacapuru Basin—(a) gridded network width functions; (b) gridded network response functions with a wave velocity of 0.32 ms^{-1} and diffusion coefficient of 99,500 m^{2}s^{-1}.*

Table 1. Comparison of volumes of generated runoff and observed flow

Year	Generated runoff mm	Observed flow mm	%underestimate
1980	1023	1143	10.5
1981	1125	1248	9.9
1982	1110	1435	22.6
1983	1123	1194	5.9
1984	1057	1406	24.8
1985	1046	1272	17.8
1986	1010	1440	29.9
1987	987	1372	28.1
1988	919	1343	31.6
average	1044	1317	20.7

but does fall within their estimate of the likely range of velocities (0.17 to 0.57 ms^{-1}). In fact, a lower value might be expected because of floodplain inundation which is treated explicitly by Vörösmarty *et al.* (1989) but is only implicit in the model used here.

Figure 3 shows the observed flows, generated runoff and routed runoff using the calibrated routing parameters. The timing of the peak runoff at Manacapurú, as determined by the spatially-cumulated generated runoff, is out of phase with the observed flow by a factor of about three months. Extrapolated to the mouth of the Amazon, the phase difference would be about six months and, given the volume of the Amazon freshwater flow, this may well affect the salinity gradients in the Atlantic and hence the global circulation. Figure 3, therefore, demonstrates the importance of river routing for making detailed comparisons between GCM output and measured flows. In this case, allowing for the underestimated runoff volumes, implementation of the routing model shows reasonably good agreement between the modelled runoff and the observed flow.

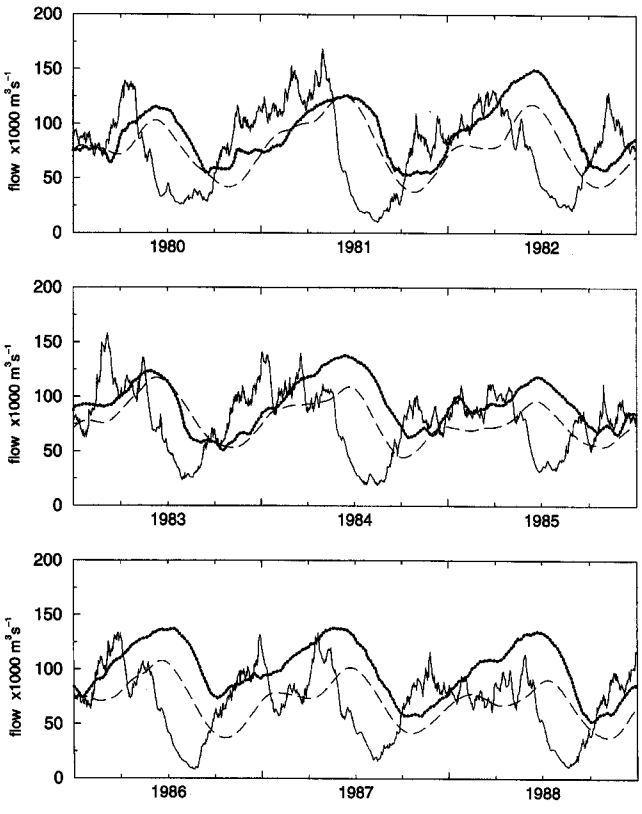

Fig. 3. *Comparison of observed flow (bold dotted line), GCM-generated runoff (solid line) and routed GCM runoff (dashed line) for the gauging station at Manacapurú.*

Estimated parameters from hydraulic geometry

When using calibrated values, the fitted routing parameters may compensate for shortcomings in the timing of runoff production, especially in cases where the runoff generation has not been, or cannot be, validated on small basins where routing has a negligible influence on the timing of the hydrological response. Consequently, it is important to be able to derive these parameters independently and, as shown above, this may be possible through channel geometry, provided there is a physical basis to the routing model.

In the case of the Amazon, there is a little published information on the hydraulic geometry of the river—notably in Oltman *et al.* (1964), Richey *et al.* (1989) and Mertes *et al.* (1996)—which can be used to estimate values of c and D using the *a priori* method derived by Robinson *et al.* (1995) outlined above. The data used are described in Table 2 and the relationships derived from these data are given below:

downstream hydraulic geometry at low water (w is channel width; d is mean channel depth):

$$w = 19.0\ Q^{0.47}\ ;\ d = 0.51\ Q^{0.30}$$

slope relationship:

$$S_0 = 1.57\ A^{-0.39}$$

Table 2a. Catchment areas and main stream lengths for the Amazon

Site	Catchment area* 10^3 km^2	Distance from Manacapurú** km
Saõ Paulo de Olivença	990	3326
Santo Antônio do Icá	1163	3477
Itapeua	1821	4290
Manacapurú	2233	4617

* from Richey *et al.* (1989)
** maximum length of channel to Manacapurú from DCW; intermediate distances calculated using thalweg distances of Mertes *et al.* (1996)

Table 2b. Hydraulic geometry at low flow for the Amazon

Site	Minimum discharge* m^3s^{-1}	Width at low water** m	Depth at low water** m	Thalweg slope** 10^{-3} mm^{-1}
Saõ Paulo de Olivença	20,000	2000	10.0	0.033
Manacapurú	70,000	3600	14.5	0.024

* from Richey et al. (1989)
** from Mertes et al. (1996)

channel length relationship:

$$\max\{L_n\} \propto A^{0.42}$$

discharge-area relationship for low flow:

$$Q = 6.73 \times 10^{-15} A^{1.54}$$

The effective rainfall rate has been assumed to be the mean observed flow (used as a surrogate for generated runoff) of 3.6 mm/day, or 4.2×10^{-8} ms^{-1}, as the flow record shows essentially a single hydrograph over the entire year. In the absence of published data, some assumptions must also be made about the at-a-station hydraulic geometry. From examples of cross-sections plotted in Oltman *et al.* (1964), two very different types of channel may be defined. One is approximated by a parabolic cross-section, with an assumed constant slope and Manning's roughness coefficient, giving a width exponent of 0.23 and a depth exponent of 0.46 (Ferguson, 1986). The other is defined as an actively eroding meandering/braided river (Mertes *et al.*, 1996) with an asymmetric cross-section in which the width increases much more rapidly than the depth with increasing flow at medium to high flows. Exponents for this type of river are given by Williams (1978) as 0.54 and 0.26 for the width and depth respectively.

Applying these two types of cross-section, Eqns. (9) and (10) give a kinematic wave velocity of between 0.30 and 0.66 ms^{-1} and a diffusion coefficient of between 42,500 and 60,500 m^{2}s^{-1}. It should be noted that the wave velocity is sensitive to $(b_1 + f_1)$, i.e. it is essentially a function of the velocity exponent, while the diffusion coefficient is only affected by the value of the depth exponent (f_1). The estimated wave velocities bracket that found by calibration and the estimated diffusion coefficients are of the same order of magnitude as the calibrated value. The fact that the calibrated velocity is near the lower limit of the estimated values and the diffusion coefficient is slightly underestimated is probably due to the fact that the estimates are based entirely on the within-channel geometry whereas the calibrated values include the effects of flood plain inundation and exchange of water between the flood plain and the main channel. These processes would tend to reduce the wave velocity and increase the diffusion coefficient compared to values which assume in-bank flows.

Figure 4 shows the observed flow and routed GCM runoff using the calibrated values and the two hydraulic geometry extremes for the period 1980–1985. It is clear that the assumption of a parabolic cross-section yields a wave velocity which is too rapid, causing early and more pronounced peaks. However, the assumption of an actively eroding meandering/braided channel provides routed runoff very similar to that using the calibrated values, suggesting that the method is not over-sensitive to small differences in the parameter values. Consistency between the calibrated and estimated values also lends support to the physical basis of the method and to the possibility of estimating parameter values *a priori*, provided there is sufficient channel geometry data on which to make these estimates. This is not only desirable as an independent means of providing parameter values but is necessary in cases where there are limited observed flows or where the volumes of GCM-generated runoff are so poor that calibration is impossible.

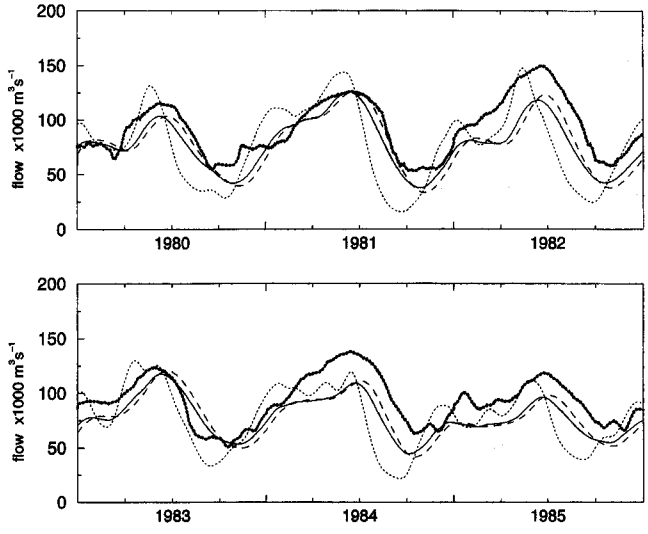

Fig. 4. *Comparison of observed flow (bold dotted line), routed GCM runoff using calibrated parameters (solid line) and estimated parameters based on an assumed parabolic cross-section (dotted line) and an actively eroding channel (dashed line).*

ARKANSAS-RED RIVER BASINS

The fact that routing generated runoff is fundamental for making detailed comparisons between GCM output and measured flows has been demonstrated in an off-line example in the case of the Amazon. The application to the Arkansas and Red River basins, within the GCIP (GEWEX Continental-scale International Project) initiative, provided the opportunity to integrate the routing within a macro-scale hydrological model operating on an

hourly time interval and using the observed meteorological forcing made available by GCIP (Kilsby *et al.*, 1998). In addition, the routing model has been implemented in such a way as to provide flows for a series of nested catchments, thus showing its potential to act as a useful tool for pinpointing *where* the modelling of generated runoff needs to be improved.

Available data

The network width functions (NWFs) were derived using the river reach data of the US Environmental Protection Agency as provided on the GCIP Reference Data Set (GREDS) CD-ROM (Rea and Cederstrand, 1994). These data are derived from cartographic sources at a scale of 1:250k. Because the hydrological model was based on a 17 km grid and the area to the west of the Arkansas and Red River basins is semi-arid, a number of additional links between grid squares had to be included manually. This was done on the basis of the USGS catchment boundaries and the network generated from a 500 m digital elevation model. The Arkansas and Red River basins cover an area of over 534,000 km^2 and there are 1923 grid squares for which NWFs and network response functions are required. The gauging stations chosen for comparison of the generated and observed runoff are Syracuse (66,800 km^2), Hutchinson (100,752 km^2), Tulsa (193,000 km^2) and Murray Dam (409,000 km^2) on the Arkansas River and Burkburnett (53,276 km^2), Gainesville (79,725 km^2) and Index (124,398 km^2) on the Red River.

Calibration of the routing model parameters was not possible due to the fine grid and large datasets of generated hourly runoff. Consequently, *a priori* estimates of the routing parameter values were calculated using the method of Robinson *et al.* (1995) and the hydraulic geometry data available in Leopold and Maddock (1953) for rivers of the Mid-West USA. The basic channel geometry data from Leopold and Maddock (1953) are for mean annual flow and have been plotted in Fig. 5. These provide the relationships given in Table 3. The network length to catchment area relationship was derived from the river network data and the catchment areas for the seven gauging stations of interest. Substituting these parameter values into Eqns. (9) and (10) gives the following equations for the effective wave velocity and diffusion coefficient:

$$c = 10.59\, A^{0.155}\, p_0^{0.34} \qquad (11)$$

$$D = 0.00568\, A^{1.01}\, p_0^{0.74} \qquad (12)$$

Model Results

The effective rainfall rate corresponding to the mean annual flow was derived from observed river flow data supplied by the USGS for the period 1979–1988 for both the Arkansas at Murray Dam and the Red River at Index. Due to the strong rainfall gradient across the basin, the effective rainfall rate for the mean annual flow at Murray Dam corresponds to an effective rainfall rate for much higher flow peaks, of the order of the mean annual flood, in the upper parts of the basin. A similar, but less pronounced, trend is seen in the Red River. However, the method adopted for calculating the catchment average c and D parameters assumes uniform rainfall and the nested routing procedures will work only if driven by the effective rainfall rate for the most downstream basin. Table 4a gives the estimated values for the wave velocity and diffusion coefficient using these effective rainfall rates and Eqns. (11) and (12). The calculated values of wave velocity are reasonable and accord with general practice, but the diffusion coefficients tend to be somewhat underestimated.

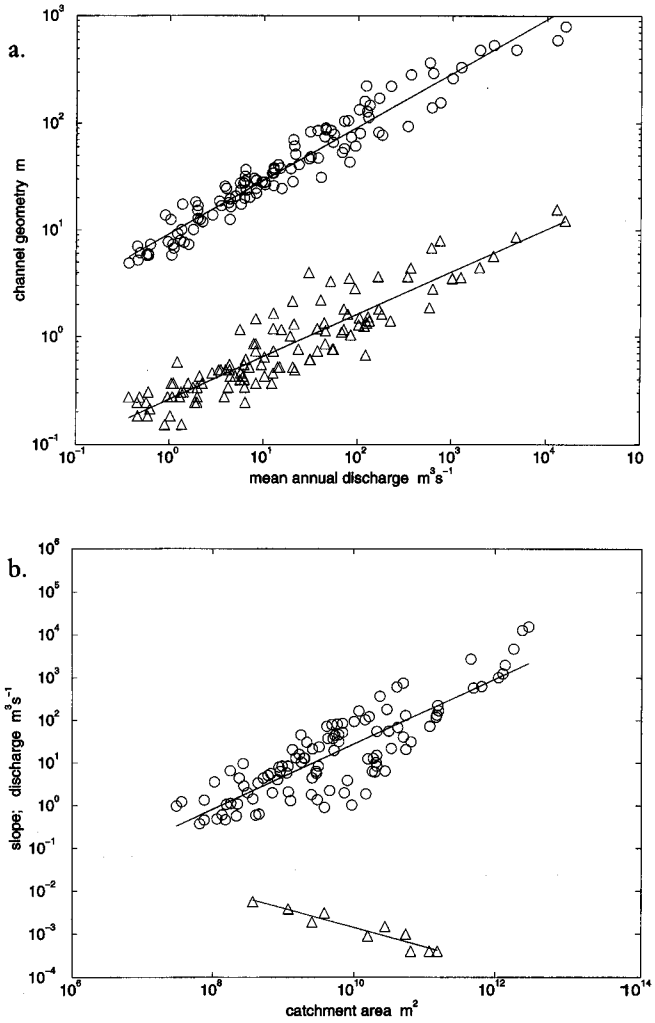

Fig. 5. *General relationships for US Mid-West rivers: a. hydraulic geometry ○ width, △ depth; b. regional discharge-area ○ and slope-area △ relationships.*

Network response functions for each of the 1923 grid squares have been calculated using these c and D values and the gridded NWFs, on the assumption that each grid square contributes to only one downstream gauge. This means that, for the nested catchments, routing parameters

Table 3. Relationships derived from data for rivers in the Mid-West USA

At-a-station channel width	$w \propto Q^{0.26}$		Leopold and Maddock (1953)
Downstream channel width	$w = 9.23\ Q^{0.50}$	$R^2 = 0.94$	Fig. 5a: data from Leopold and Maddock (1953)
At-a-station channel depth	$d \propto Q^{0.40}$		Leopold and Maddock (1953)
Downstream channel depth	$d = 0.26\ Q^{0.40}$	$R^2 = 0.83$	Fig. 5a: data from Leopold and Maddock (1953)
Slope-Area relationship	$S_0 = 40.3\ A^{-0.45}$	$R^2 = 0.89$	Fig. 5b: data from Leopold and Maddock (1953)
Mean annual flow-Area relationship	$Q = 6.2 \times 10^{-7}\ A^{0.77}$	$R^2 = 0.73$	Fig. 5b: data from Leopold and Maddock (1953)
Network length-Area relationship	$\max\{L_n\} \propto A^{0.59}$	$R^2 = 0.85$	Data from US EPA river reach files and areas for selected gauging stations

Table 4a. A priori effective parameters for river routing on the Arkansas and Red Rivers

	Effective wave velocity ms^{-1}	Effective diffusion coefficient m^2s^{-1}
Arkansas River		
Syracuse (66,800 km²)	0.65	252
Hutchinson (100,752 km²)	0.70	381
Tulsa (193,000 km²)	0.77	735
Murray Dam (409,000 km²)	0.86	1570
Red River		
Burkburnett (53,276 km²)	0.62	191
Gainesville (79,725 km²)	0.66	287
Index (124,398 km²)	0.70	450

Table 4b. Effective parameters for joining stretches of main river

	Effective wave velocity ms^{-1}	Effective diffusion coefficient m^2s^{-1}
Syracuse to Hutchinson (440 km)	0.74	493
Hutchinson to Tulsa (432 km)	0.94	1322
Tulsa to Murray Dam (527 km)	1.20	3557
Burkburnett to Gainesville (245 km)	0.72	412
Gainesville to Index (530 km)	0.75	623

must be calculated for the joining stretch of main channel for use in Eqns. (6) and (7). The methods used follow the assumptions behind the calculation of the effective parameters. Thus, the effective value of c for the joining reach was calculated on the basis of the time dimension; in other words, how much quicker does the flow peak have to travel through the joining reach to make up for the smaller wave velocity in the upstream catchment. Values of D were calculated as a weighted average based on the mainstream length in the respective catchments. The values obtained were checked by comparing the network response function for the entire catchment with that produced using the separate components of the upstream and downstream catchments and the joining channel. The resulting effective parameters for the joining stretches of main channel are given in Table 4b. It will be noted that the effective values are higher than the corresponding catchment values because of the need to offset the effect of the upper catchment. The overall response functions for each of the seven catchments, as derived from the gridded network response functions and the joining stretches of main river, are shown in Fig. 6.

Figure 7 shows the results of implementing the routing model described above in the UP model (Kilsby *et al.*, 1999). The spatially-cumulated runoff (solid line), routed runoff (dashed line) and 'observed' flow (thick dotted line) are shown for the two more downstream sites on the Arkansas and for the lowest site on the Red River. In the case of the Arkansas, naturalised flows were provided by the US Army Corps of Engineers, Tulsa District. In the case of the Red River, naturalised flows were not available and observed flows which include the effects of regulation are shown. In each of the three cases, the generated runoff volumes underestimate the observed flows. Over the period shown, this amounts to 0.2% for Tulsa (compared to naturalised flows at the more upstream point of Ralston), 28% for Murray Dam and 36% for Index. These

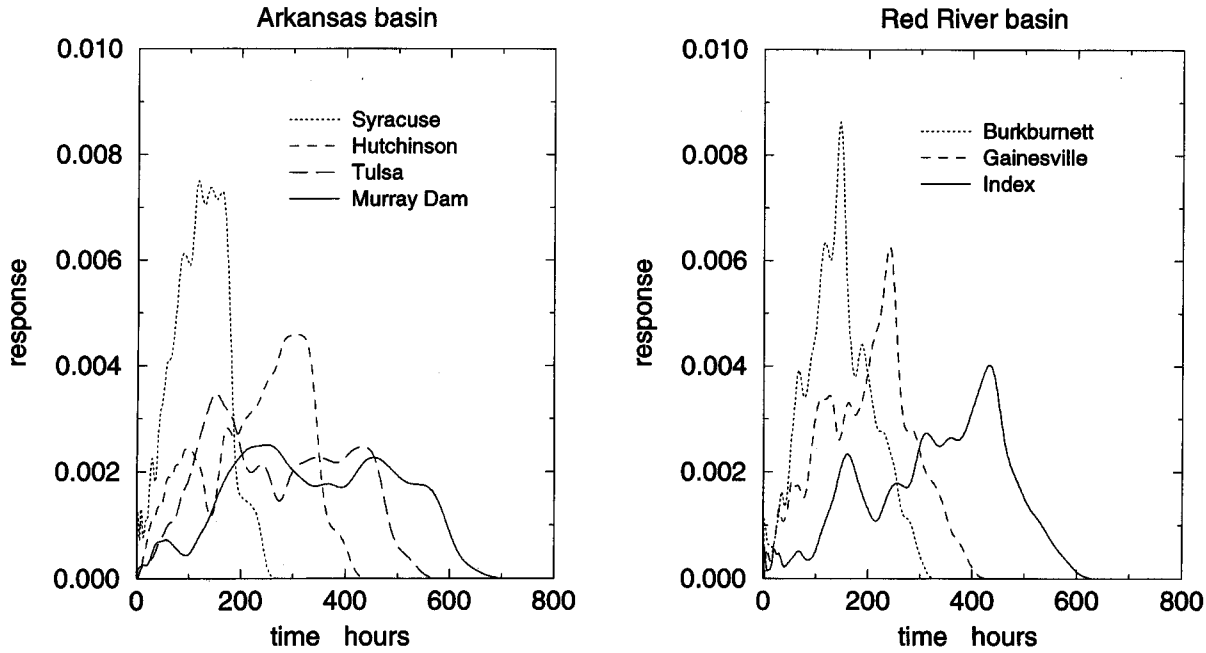

Fig. 6. *Network response functions for subcatchments of the Arkansas and Red River basins.*

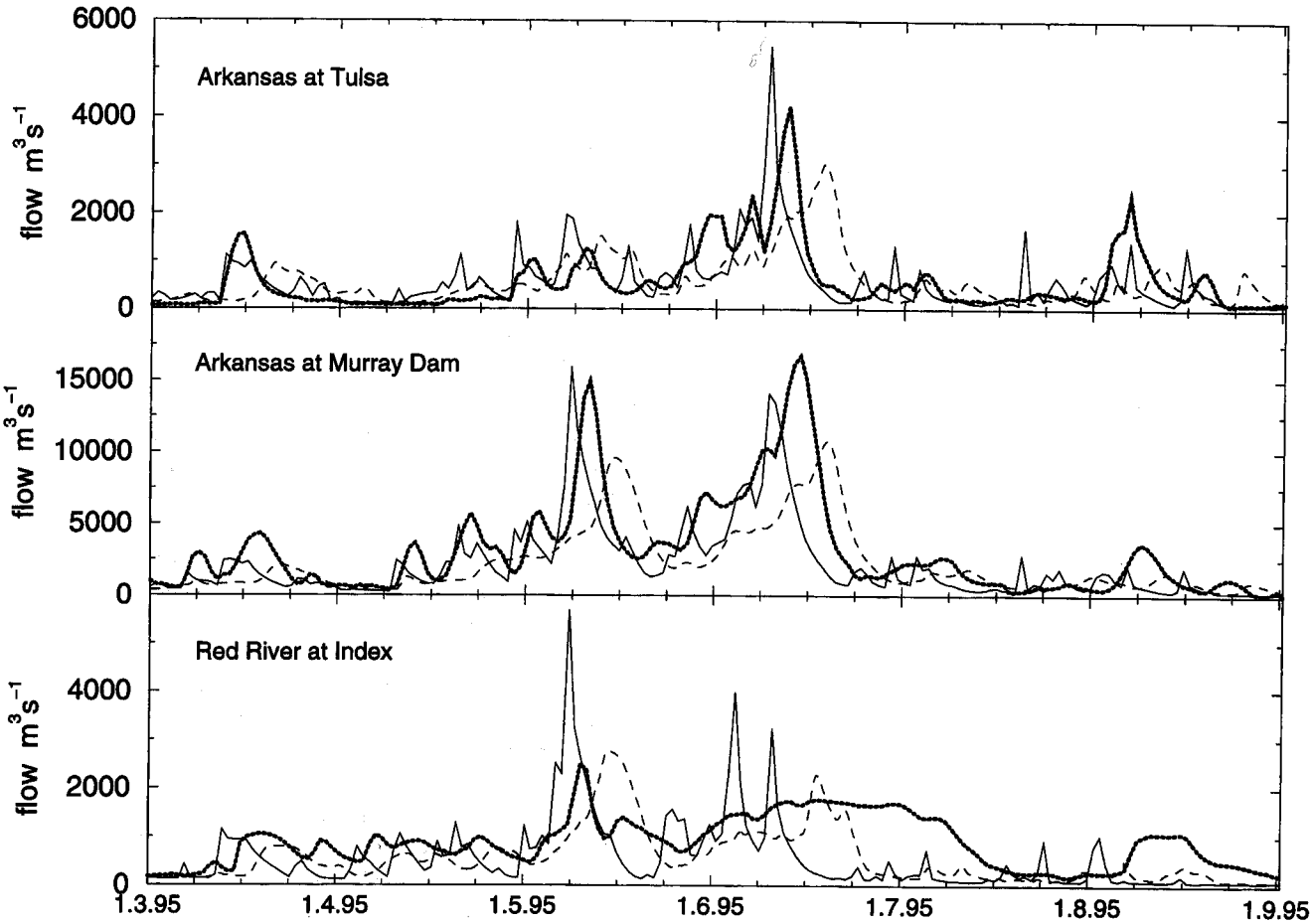

Fig. 7. *Generated runoff (solid line), routed runoff (dashed line) and 'observed' flow (thick dotted line) for the Arkansas and Red Rivers; naturalised flows are shown for the Arkansas.*

flow volumes are not as accurate as those generated by the highly calibrated model of Abdulla and Lettenmaier (1997), but it should be borne in mind that the UP model is more physically based (Ewen *et al.*, 1999) and has a much more limited calibration.

It is clear from Fig. 7 that, in the case of the Arkansas at both Tulsa and Murray Dam, the river routing employed gives much more delayed peaks than those shown by the naturalised flows. While the assumptions behind the naturalisation of the flows are unknown and it is difficult to separate out the effects of the timing of runoff generation and routing at this scale, given the influence of groundwater flow (Kilsby *et al.*, 1999), the evidence suggests that it is probably the routing which is at fault. For example, if one looks at the June peak for Tulsa and its counterpart at Murray Dam, the lag in the naturalised flows is about two days while that for the routed flow is about four days. Similarly, assuming that the generated runoff has the correct timing, the naturalised flows suggest a within-river delay of about three days for Tulsa and five days for Murray Dam, whereas the routing used here provides delays of five and nine days respectively. These delays are consistent with the estimated velocities and the distance between each gauging station and the peak in its network width function. Consequently, to match the naturalised flows, velocities should be approximately twice the estimated velocities. High wave velocities would be consistent with large differences between flood peaks and baseflows (e.g. flash floods in semi-arid areas) and with canalisation of the main river channel. It should also be noted that the recession limbs are of a similar shape in both the routed and naturalised flows suggesting that the values of D are not unreasonable. Again low values of D would be consistent with canalised flows.

In the case of the Red River, even using the observed flows, it can be seen that the routing model tends to produce too much of a delay on the hydrograph, although the overall magnitude of the main flow peak is of the right order. However, the hydrograph shapes are indicative of substantial flow regulation and the lack of naturalised flows in this case precludes a full assessment of the routing model. It does, however, raise the question, within the context of global climate modelling, as to how far man-made influences on flow regime need to be included to provide realistic timing of ocean inflows. For validating GCMs, use of naturalised flow data, if available, will suffice.

Discussion

Flow regulation within the Mississippi basin makes an assessment of the routing model difficult, although the availability of naturalised flows for the Arkansas has made comparisons possible. The difficulty of separating the timing of runoff production and routing is also acknowledged. However, the UP modelling system was calibrated on a limited number of small catchments with diverse characteristics. These showed good agreement with gauged flows in cases where the influence of routing is negligible. Thus, there is some confidence in the timing of runoff production. Similarly, because of the relatively fine grid scale, the spatial production of runoff is much better defined compared to GCM data and the use of rainfall radar data on an hourly time step provides good spatial and temporal definition in terms of the dominant driving variable. It has, therefore, been concluded that it is the routing which provides too much of a delay in the modelled runoff. The main reason for this is thought to lie in the use, in Eqns (11) and (12), of an effective rainfall rate derived from the mean annual flow. As there are distinct hydrograph peaks in the case of the Arkansas and Red Rivers, this assumption is less justified than in the case of the Amazon. Furthermore, if a rainfall rate consistent with the peak flows seen in Fig. 7 is used, then the estimated wave velocity can be approximately doubled to 1.2 ms^{-1} for Tulsa and 1.6 ms^{-1} for Murray Dam. The value of D would also increase to more reasonable values for basins of this size (1755 m^2s^{-1} for Tulsa and 6000 m^2s^{-1} for Murray Dam). Given the sensitivity of c and D to the choice of effective rainfall rate, further exploration of the range of possible values and their effect on the routing parameters should be considered. Other points regarding the *a priori* estimation of the routing parameters are discussed below.

Firstly, it should be noted that two differences stand out between the derivations given here and those of Robinson *et al.* (1995). One is that, in this case, the hydraulic geometry at the mean annual flow, rather than bankfull, has been used in the calculations. Although this has been used consistently with a regional mean annual flow-area relationship, the downstream hydraulic geometry does assume that the mean annual flow has a consistent frequency of occurrence throughout the basin. Flow estimates are given for different return periods for a number of stations in Kansas by Jordan (1986) and, if these are used with suitable adjustments to the downstream hydraulic geometry, the resulting estimates of the wave velocity and diffusion coefficient are very similar. This, therefore, reinforces the original results, stressing the use of consistent relations rather than a particular frequency of occurrence.

The other major difference between the parameters in this study and those found by Robinson *et al.* (1995) for the Hutt catchment lies in the slope-area relationship. The diffusion coefficient is highly dependent on this but it plays no part in estimating the wave velocity. The slope-area relationship in this case has been estimated on the basis of only ten points from Leopold and Miller (1953); these are all on river reaches with a catchment area of over 500 km^2. It is therefore likely that this does not reflect the overall slope-area relationship of the basin. The exponent of –0.45 is rather more than the –0.6 often quoted (Hack, 1957) and more than the value of –0.75 which represents a balance between uniform frictional loss and minimisation

of total work (Richards, 1982). However, the effect on D of decreasing the exponent will be offset by a concomitant increase in the coefficient. It is, therefore, unclear, without additional data, how the estimate of D might change.

Finally, it is also worth revisiting the assumptions which Robinson *et al.* (1995) make in moving from single estimates of c and D to the effective values for an entire river network. Assumptions of homogeneity of rainfall and a rectangular network width function were both made to force an analytical solution. Neither of these assumptions hold for the Arkansas and Red River basins. To get around these assumptions, the effective parameters should be determined by numerical integration over the observed network width function, perhaps weighted by the rainfall distribution (cf. Naden, 1992). The results of Robinson *et al.* (1995) suggest that the network average value for c is about half that of the outlet river reach while the average value for D is only fractionally less than the value for the outlet river reach. If these results are found to be generally applicable, there is scope for developing this routing method globally with a minimum amount of information on channel geometry, or perhaps using remote sensing to provide the required parameters from an analysis of water waves, from radar altimetry, as they pass through the downstream reaches of major rivers.

Concluding remarks

This paper has presented the application of a physically-based method for routing generated runoff through continental-scale catchments using available river network data from cartographic sources and published channel geometry data.

The method gives good results in the case of an off-line test of GCM-generated runoff against observed flow on the scale of the Amazon at a daily time interval. Digital network data were derived from the Digital Chart of the World and the sensitivity of the method to different assumptions about the channel geometry has been illustrated. The application of the method to the Arkansas and Red River basins within a macro-scale hydrological model operating on a 17 km grid using nested catchments has also been presented. In this case, the network width functions were calculated from the US EPA river reach data. Routing parameters were estimated using published channel geometry data. Naturalised flows suggested that initial estimates were too low but that these might be corrected by using a different effective rainfall rate, consistent with the individual hydrographs rather than that derived from the mean annual flow.

Further work is needed to elucidate the necessary scale of global river network data for the purpose of routing and to improve the estimation of routing parameters based on channel geometry. In particular, this should explore how to determine a useful effective rainfall rate. It should also include the numerical integration of cross-section c and D values using weights from the observed network width function and a relaxation of the assumption of uniform rainfall. An assessment of how well routing parameters can be estimated, in the absence of calibration, should also be made using both hydraulic geometry and remote sensing across a wide range of basins. This requires use of more accurate generated runoff than that used here.

Notwithstanding these comments, it is clear that river routing is necessary for the comparison of generated runoff and observed river flows and for the correct timing of runoff into the world's oceans. The method adopted here is physically based and incorporates both the effect of geomorphological dispersion through the use of the network width function and hydraulic dispersion through the use of the convective-diffusion equation. It, therefore, offers substantial advantages over existing methods which use either grid-to-grid box routing or a simple advection velocity. Given the possibility of *a priori* parameter estimation and the ability to use globally-available data, it provides a promising method for future development and application at GCM and continental scales.

Acknowledgements

The authors acknowledge the financial support provided by the Natural Environment Research Council through its TIGER (Terrestrial Initiative in Global Environmental Research) Programme; award number T91/83. Thanks are also due to DNAEE and ORSTOM for flow data for the Amazon, MSSL for the loan of the hydrographic charts for the Amazon, USGS for flow data for Arkansas and Red Rivers; UK Met. Office for use of Hadley Centre GCM output; USGS and UCL for network data for the Amazon; the Tulsa District Office of the US Army Corps of Engineers and Princeton University for naturalised flows for the Arkansas River.

References

Abdulla, F.A. and Lettenmaier, D.P., 1997. Application of regional parameter estimation schemes to simulate the water balance of a large continental river. *J. Hydrol.*, **197**, 258–285.

Abramowitz, M. and Stegun, I.A., 1965 *Handbook of mathematical functions.* Dover Publications Inc., New York, USA, 1046 pp.

Beven, K. and Wood, E.F., 1993. Flow routing and the hydrological response of channel networks. In *Channel Network Hydrology*, K. Beven and M.J. Kirkby (eds.), Wiley, Chichester, UK, 99–128.

Birkett, C.M., 1998. Contribution of the TOPEX NASA radar altimeter to the global monitoring of large rivers and wetlands. *Wat. Resour. Res.*, **34**, 1223–1239.

Denko, D., 1992 *Digital Chart of the World*, Geodata.

Dooge, J.C.I., 1973. *Linear theory of hydrologic systems*, Technical Bulletin 1468, United States Department of Agriculture, Washington, US, 327 pp.

Dümenil, L., Isele, K., Liebscher, H.-J., Schröder, U., Schumacher, M. and Wilke, K., 1993. *Discharge Data from 50*

selected rivers for GCM validation, Report No. 100, Max-Planck-Institut für Meteorologie, Hamburg, 66 pp.

Eagleson, P.S., 1970. *Dynamic Hydrology*, McGraw Hill, New York, 462 pp.

Ewen, J., Sloan, W.T., Kilsby, C.G. and O'Connell, P.E., 1999. The UP modelling system for large-scale hydrology: deriving large-scale physically-based parameters for the Arkansas-Red River basin, *Hydrol. Earth System Sci.*, **3**, 125–136.

Ferguson, R.I., 1986. Hydraulics and hydraulic geometry, *Prog. Phys. Geog.*, **10**, 1–31.

Franchini, M. and O'Connell, P.E., 1996. An analysis of the dynamic component of the geomorphologic instantaneous unit hydrograph. *J. Hydrol.*, **175**, 407–428.

Franchini, M. and Todini, E., 1989. PABL: *A parabolic and back-water scheme with lateral inflow and outflow*. Fifth IAHR Int. Symp. on Stochastic Hydraulics, Report No. 10, Institute for Hydraulic Construction, University of Bologna.

Gustard, A., 1994. A review of the FRIEND research programme in western and northern Europe. In *FRIEND: Flow regimes from international experimental and network data*, P. Seuna, A. Gustard, N.W. Arnell, and G.A. Cole (eds.), International Association of Hydrological Sciences Publication No. 221, Wallingford, UK, 3–10.

Hack, J.T., 1957. Studies of longitudinal stream profiles in Virginia and Maryland. *USGS Professional Paper 294B*, Washington, USA, 97 pp.

Hall, C.D., Stratton, R.A. and Gallini, M.L., 1995. *Climate simulations with the unified model AMIP runs*, CRTN1, UK Met. Office, Bracknell, UK, 84 pp.

Jordan, P.R., 1986. Magnitude and frequency of high flows of unregulated streams in Kansas, *US Geol. Surv. Wat. Supply Pap. 2280*, Washington, USA, 35 pp.

Kilsby, C.G., Ewen, J., Sloan, W.T., Burton, A., Fallows, C.S. and O'Connell, P.E., 1999. The UP modelling system for large-scale hydrology: simulation of the Arkansas-Red River basin, *Hydrol. Earth System Sci.*, **3**, 137–149.

Kirkby, M.J., 1976. Tests of the random network model, and its application to basin hydrology. *Earth Surface Processes*, **1**, 197–212.

Kuhl, S.C. and Miller, J.R., 1992. Seasonal river runoff calculated from a global atmospheric model, *Wat. Resour. Res.*, **28**, 2029–2039.

Leopold, L.B. and Maddock Jr, T., 1953. The hydraulic geometry of stream channels and some physiographic implications. *US Geol. Surv. Prof. Pap. 252*, Washington, USA, 57 pp.

Liston, G.E., Sud, Y.C. and Wood, E.F., 1994. Evaluating GCM land surface hydrology parameterizations by computing river discharges using a runoff routing model: application to the Mississippi basin. *J. App. Meteorol.*, **33**, 394–405.

Lohmann, D., Nolte-Holube, R. and Raschke, E., 1996. A large-scale horizontal routing model to be coupled to land surface parametrization schemes, *Tellus*, **48A**, 1–14.

Mertes, L.A.K., Dunne, T. and Martinelli, L.A., 1996. Channel-floodplain geomorphology along the Solimões-Amazon River, Brazil, *Geol. Soc. Am. Bull.*, **108**, 1089–1107.

Mesa, O.J. and Mifflin, E.R., 1986. On the relative role of hillslope and network geometry in hydrologic response. In *Scale Problems in Hydrology*, V.K. Gupta, I. Rodriguez-Iturbe and E.F. Wood (eds.). D. Reidel Publishing Co., Dordrecht, The Netherlands, 1–17.

Miller, J.R., Russell, G.L. and Caliri, G., 1994. Continental-scale river flow in climate models. *J. Climate*, **7**, 914–928.

Naden, P.S., 1992. Spatial variability in flood estimation for large catchments: the exploitation of channel network structure. *Hydrol. Sci. J.*, **37**, 53–71.

Naden, P.S., 1993. A routing model for continental-scale hydrology. In *Macroscale modelling of the hydrosphere*, W.B. Wilkinson (ed.), International Association of Hydrological Sciences Publication No. 214, Wallingford, UK, 67–79.

Nijssen, B., Lettenmaier, D.P., Liang, X., Wetzel, S.W. and Wood, E.F., 1997. Streamflow simulation for continental-scale river basins. *Wat. Resour. Res.*, **33**, 711–724.

Oki, T., Kanae, S. and Musiake, K., 1996. River routing in the global water cycle, *GEWEX News*, **6**, 4–5.

Oltman, R.E., Sternberg, H. O'R., Ames, F.C. and Davis Jr, L.C., 1964. Amazon River Investigations Reconnaissance Measurements of July 1963, *US Geol. Surv. Circ. 486*, US Dept. of the Interior, Washington, 15 pp.

Rea, A. and Cederstrand, J.R., 1994. *GCIP Reference Data Set (GREDS) CD-ROM*, U.S. Geological Survey Open-file Report 94–388.

Richards, K.S., 1982. *Rivers: form and process in alluvial channels*, Methuen, London, 358 pp.

Richey, J.E., Mertes, L.A.K., Dunne, T., Victoria, R.L., Fosberg, B.R., Tancredi, A.C.N.S. and Oliveira, E., 1989. Sources and routing of the Amazon river flood wave, *Global Biogeochemical Cycles*, **3**, 191–204.

Rinaldo, A., Marani, A. and Rigon, R., 1991. Geomorphological Dispersion. *Wat. Resour. Res.*, **27**, 513–525.

Robinson, J.S., Sivapalan, M. and Snell, J.D., 1995. On the relative roles of hillslope processes, channel routing, and network geomorphology in the hydrologic response of natural catchments. *Wat. Resour. Res.*, **31**, 3089–3101.

Russell, G.L. and Miller, J.R., 1990. Global runoff calculated from a global atmospheric general circulation model. *J. Hydrol.*, **117**, 241–254.

Sausen, R., Schubert, S. and Dümenil, L., 1994. A model of river runoff for use in coupled atmosphere-ocean models. *J. Hydrol.*, **155**, 337–352.

Snell, J.D. and Sivapalan, M., 1994. On geomorphological dispersion in natural catchments and the geomorphological unit hydrograph. *Wat. Resour. Res.*, **30**, 2311–2323.

Snell, J. and Sivapalan, M., 1995. Application of the meta-channel concept: construction of the meta-channel hydraulic geometry for a natural channel. *Hydrol. Processes*, **9**, 485–505.

Sutcliffe, J.V. and Parks, Y.P., 1989. Comparative water balances of selected African wetlands. *Hydrol. Sci. J.*, **34**, 49–62.

Tauveron, N., 1996. *Application of a simple river routing model to the Amazon basin and its use for validating GCM output against measured flow data*, Unpublished thesis for École Polytechnique Promotion X-93.

Todini, E., 1996. The ARNO rainfall-runoff model, *J. Hydrol.*, **175**, 339–382.

van de Nes, Th.J., 1973. *Linear analysis of a physically-based model of a distributed surface runoff system*. Centre for Agricultural Publishing and Documentation, Wageningen, The Netherlands, 104 pp.

van der Leeden, F., Troise, F.L. and Todd, D.K., 1990. *The Water Encyclopedia*, 2nd. edition, Lewis Publishers Inc., Michigan, USA, 808 pp.